Probability of hotspot ignition in turbulent hydrogen-air mixtures using Direct Numerical Simulations

Gábor Janiga*, Gordon Fru**, Abouelmagd Abdelsamie, Dominique Thévenin

Laboratory of Fluid Dynamics and Technical Flows, University of Magdeburg "Otto von Guericke", Universitätsplatz 2, D-39106 Magdeburg, Germany

Abstract

Direct Numerical Simulations (DNS) of stoichiometric H_2-air mixtures have been performed to investigate the probability of safety-relevant ignition processes under both laminar and turbulent conditions. For the range of parameters considered, the computed induction times show a very good agreement with experimental data. DNS show that all spherical kernels with initial temperatures and radii larger than the critical values will successfully ignite the stoichiometric premixed H_2-air system and lead to a self-sustained flame as long as the turbulence intensity remains below a given threshold, here $u'/s_L < 3.1$ (where u' and s_L are the rms velocity and the laminar flame speed, respectively). Beyond this value, the mean ignition delay becomes rapidly higher (up to 50%) than the laminar one for all setups that lead to successful ignition, but an increasing percentage of all cases lead to misfires. Ultimately, a misfire becomes systematic around $u'/s_L > 7.5$.

Introduction

The physicochemical processes leading to ignition of a reactive mixture have been extensively investigated during the last decades, demonstrating both the importance and the complexity of this issue. Most early studies of ignition phenomena from the point of view of safety analysis could only rely on experimental measurements and simplified theoretical models, like those reported in the seminal textbook of Lewis and von Elbe [1] (first published in 1951). This is due to the fact that ignition is a fully coupled process involving two main aspects of very high complexity: 1) chemistry and 2) heat transfer, both mostly in a turbulent environment.

Chemical kinetics describe the evolution of all radicals needed for the onset of ignition. A quantitative investigation taking this point into account can only be realized if all chemical pathways are known, if the corresponding reaction parameters have been determined accurately, and if the available computational power is sufficient to carry out corresponding simulations, involving possibly hundreds or thousands of individual reactions. The challenge associated with this issue hence completely depends on the composition of the considered mixture, in particular on the fuel. This is why the present study only considers stoichiometric hydrogen-air mixtures, for which accurate and validated physicochemical data are available [2].

Secondly, heat exchange processes with the surroundings will be essential to decide if the ignition event will be successful and lead to a fully developed flame, or if it will fail after a short time. In order to take this aspect into account, all relevant heat exchange paths (convection and conduction) must be described accurately. A reliable quantitative study then necessitates an excellent description of the local turbulent flow conditions and of all relevant transport properties (in particular diffusion). The challenges associated with this second aspect depend on the flow conditions (laminar vs. turbulent) and on the retained configuration (premixed vs. non-premixed, possible interaction with surfaces, possible importance of radiative heat transfer or of evaporation).

In the present work, only premixed ignition is considered. Due to the progress in computing power, simulations taking into account in a realistic manner the surrounding turbulent flow conditions, and thus the convective and conductive heat exchange, became possible in the early nineties. Corresponding results are found for instance in [3, 4], for two-dimensional (2D) flows and/or employing a single-step chemical reaction. The obtained observations have been discussed further in [5, 6], demonstrating in particular the interest of Direct Numerical Simulations (DNS) to investigate such configurations. Nevertheless, the probability of successful ignition could not be considered using DNS and realistic chemical kinetics at this early stage. Later works went a step ahead to consider more realistic kinetics in 2D flows (e.g., [7]) or in three-dimensional (3D) conditions but with a simplified kinetic description (one-step chemistry, like for instance in [8, 9, 10]). Recent DNS studies indeed consider 3D flames with complex kinetic schemes (see e.g., [11]) but do not investigate specifically ignition processes. In the context of hot-gas jet ignition, 2D numerical studies of the combustion of lean premixed natural gas-air mixtures are reported in [12] where the influence of variations in ignition energy, affected by both kernel temperature and size, and equivalence ratio, on the flame development is studied in an

*Corresponding author. Fax: +49 391 67 12 840

**Now by GexCon AS, R&D, Norway

Email addresses: janiga@ovgu.de (Gábor Janiga), gordon.fru@ovgu.de (Gordon Fru), abouelmagd.abdelsamie@ovgu.de (Abouelmagd Abdelsamie), thevenin@ovgu.de (Dominique Thévenin)

initially quiescent gas. It is shown that as long as the available ignition energy is greater than a minimum, the duration in which a steady flame speed is achieved is a strong function of kernel temperature; it is not a function of kernel size. More recently, a parametric study of auto-ignition scenarios for lean n-heptane/air [13] and hydrogen/air [14] mixtures with thermal stratification at constant volume and high pressure have also been conducted using detailed 2D DNS. Unlike the focus here, the study concentrates on the influence of imposed initial temperature fluctuations (T') and the ratio of turbulence to ignition delay timescale on the auto-ignition of the lean mixture.

The present study relies exclusively on DNS with detailed chemical and transport models to investigate ignition events in turbulent premixed flames burning hydrogen, similar in configuration to those conducted in [12]. The aforementioned two aspects have been taken into account simultaneously. Configurations where autoignition is obtained in the absence of any external flow are afterwards perturbed by adding turbulent fluctuations of increasing intensity. The impact of turbulence is quantified in a statistically meaningful manner by repeating these DNS simulations, leading to independent realizations.

Problem configuration and initialization

DNS has emerged over the last two decades to provide as far as possible an exact solution for both fluid dynamics and flame structures in reacting flows.

In the present study, the massively parallel DNS flame solver *parcomb* is used, improved during more than fifteen years based on the original 2D version [15]. It solves the full compressible reactive Navier-Stokes system coupled with detailed physicochemical models. The balance equations for mass, momentum, total energy and all mass fractions are solved in a coupled manner using a sixth-order central differencing scheme on a Cartesian grid [16]. Numerical dissipation is further reduced and stability improved with the implementation of the skew-symmetric formulation [17] for the convective terms. An explicit fourth-order Runge-Kutta time integrator is employed. The extended Navier-Stokes Characteristic Boundary Conditions (NSCBC [18]) are used, with non-reflecting boundaries and pressure relaxation applied along all open faces. The parallelization relies on a 3D block structure using the Message Passage Interface paradigm for data exchange. The code offers a good single-core performance and a near perfect parallel scaling for full three-dimensional production runs.

With *parcomb*, an equation is solved explicitly for each and every chemical species involved in the employed detailed chemical scheme, simultaneously with the Navier-Stokes equations. A complex chemical reaction scheme comprising N_s species and N_r elementary reactions is considered.

For the results presented later, a H_2/O_2 chemical scheme specifically developed to investigate auto-ignition [19] has been systematically employed. It involves 38 elementary reactions and 9 species (H_2, O_2, H_2O, H, O, OH, HO_2, H_2O_2 & N_2).

Detailed models are also employed for the computations of the diffusive processes.

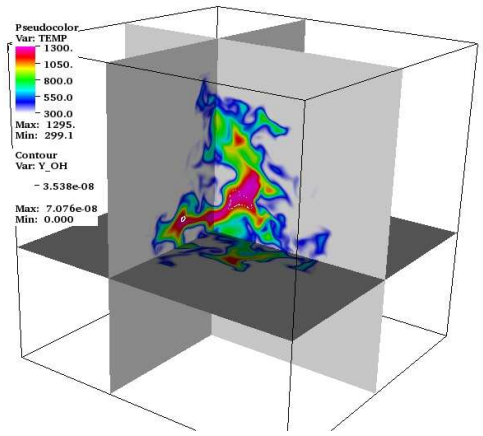

Figure 1: Typical computational domain and flame configuration for setup *S2(3)D*.

Full multicomponent diffusion velocities may be quite expensive to compute in practical simulations, since one has to determine iteratively the binary diffusion coefficients via the diffusion matrix [20]. For the present computations, we consider the Hirschfelder-Curtiss approximation [21], whereby a mixture-averaged diffusion coefficient, D_i^* for the species i in the local mixture is given as

$$D_i^* = \frac{(1 - Y_i)}{\sum_{k=1,k\neq i}^{N_s} (X_i / \mathcal{D}_{ik})} \tag{1}$$

where $\mathcal{D}_{ik}$ is the binary diffusion coefficient. In order to ensure mass conservation, the diffusion velocity $\mathbf{V}_i$ for species i is divided into a predictor and a corrector term.

Flame configurations and initialization

To validate the above numerical and physicochemical models specifically for auto-ignition studies, homogeneous configurations were first considered. In this first instance (referred hereafter as setup *S0D*), uniform initial profiles for all variables are imposed at $t = 0$ and allowed to iterate in a zero-dimensional simulation. In this way, the auto-ignition delay (or induction) times τ are obtained as a function of the mixture composition (described by the equivalence ratio Φ), and initial temperature T_0. In the second validation test case (referred hereafter as setup *S1D*), initial profiles are prescribed as above in a one-dimensional configuration but this time with a step in the middle of the domain for temperature (and hence density under initially isobaric conditions). The step is approximated by an hyperbolic tangent function involving a stiffness parameter. Checking the influence of this parameter, it is possible to find a range in which it does not show any influence on the obtained results, as seen later when comparing the results obtained for τ from setups *S0D* and *S1D*. Keeping now this stiffness parameter constant, the induction times can be parameterized and investigated as a function of the temperature peak T_0 and radius of the initial hot temperature zone, R_0. The surrounding mixture is always kept at $T_u = 300$ K.

Cases	u'/s_L	τ (ms)	Re_t
2	2.5	0.64	146
4	3.8	0.42	219
6	5.0	0.32	292
8	6.3	0.25	365
10	7.5	0.21	438
12	8.8	0.18	511
14	10.0	0.16	584

Table 1: Initial turbulence parameters for selected cases of setup *S2D*.

After successful validation, initially perfectly circular/spherical laminar premixed H_2-air kernels at $\Phi = 1.0$ are considered. The simulated domain is exemplified in Fig. 1, consisting of a square (in 2D – setup *S2D*) or cube (in 3D – setup *S3D*) of side length $L = 1.6$ cm discretized with a uniform grid spacing of 20 μm, necessary to resolve correctly the smallest vortical structures but also stiff intermediate radicals like H_2O_2.

The initial kernel is laminar, at temperature T_0 and radius R_0, located at the center of the domain and surrounded by a fresh atmospheric H_2-air mixture at T_u. The initial mass fractions $Y_{H_2} = 0.0291$ and $Y_{O_2} = 0.233$ at T_u, and $Y_{H_2O} = 0.243$ at T_0 are systematically prescribed outside and within the kernel, respectively. In all setups and cases, an appropriate nitrogen complement is added everywhere at the start.

For all turbulent cases in setup *S2(3)D*, the initial laminar profiles are superimposed with a homogeneous isotropic turbulent field at $t = 0$, generated by the digital filtering technique initially proposed in [9]. The adaptation of this technique for time-decaying turbulence in a box using *parcomb* has been discussed in [16]. For the turbulent computations presented later, the integral length scale measured directly from the initial turbulence field is kept constant and equal to $l_t = 1.27$ mm, the fresh mixture viscosity is constant as well, $\nu = 1.74\,10^{-5}$ m^2/s. Fifteen turbulence levels (one laminar case and fourteen cases with increasing turbulent velocity) have been considered, ultimately spanning a range in turbulence intensities from $u'/s_L = 1.25$ to $u'/s_L = 10.0$. The corresponding turbulent Reynolds numbers based on the integral scale $\mathrm{Re}_t = u' l_t/\nu$ increase from 73 to 584. More details are given in Table 1 for half of the turbulent cases in the interest of space.

In order to obtain statistically meaningful results, an average over a sufficient number of independent realizations is needed [22]. For this reason, up to twenty realizations have been finally considered for each turbulence intensity. Since a random number generator is involved, each DNS is associated with the same global properties of turbulence (spectrum, correlations, fluctuations, Reynolds number...) but corresponds to a different initial condition in space, and thus to a different realization. As will be shown later, a sufficiently rich DNS database might be needed to rule out spurious effects and to obtain a safer confidence interval for ignition probability of such flammable mixtures.

For most computations, our local Linux-based PC-cluster (Opteron quad-core nodes, 32 GB memory/node and Infiniband connection) involving 512 computing cores has been employed in a single-user mode. While a typical 3D computation requires about 20 days of CPU until ignition or misfire, a DNS in 2D can be finished in less than one day, allowing systematic computations.

Numerical results and discussion

First, self-ignition results in the laminar regime for the three setups are discussed. The employed physicochemical and numerical models can be validated in this manner by comparison with available experimental data. This study also delivers critical auto-ignition parameters in the absence of turbulence. Ignition delay times in two and three dimensions are then investigated and compared, showing that 2D DNS are sufficient to investigate the present problem. Finally, ignition events in the presence of turbulent fluctuations at increasing intensities and their influence on the auto-ignition delay time is discussed. Results are presented in a statistical manner towards characterizing successful ignition (or misfire) events relevant to safety issues.

There are many criteria with which the auto-ignition delay of a flammable mixture can be defined: for instance based on the moment of fastest temperature rise; fastest gas expansion; fastest pressure rise; fastest reaction rate rise; fastest rise in a given species [23, 24]... All these definitions have convincing justifications depending on the particular focus of the study, although a disparity of up to 20% in the obtained delay times might be observed [25]. When considering detailed chemistry simulations, the auto-ignition delay computed as the time of fastest temperature rise is often recommended [25]. It is used systematically in the present study.

Auto-ignition under laminar conditions

Several laminar computations (involving setups *S0D* and *S1D*) were carried out for $0.1 \leq \Phi \leq 1.0$, $0.2 \leq R_0 \leq 5.0$ mm) and $910 \leq T_0 \leq 1200$ K at one atmosphere. The dependency of τ on these parameters is presented in Fig. 2. Experimental self-ignition delay data from the literature [26, 27] for different T_0 and Φ within the limits considered in the simulations have been included as well in Fig. 2. For all conditions, the numerical results from setup *S0D* show an excellent agreement with the corresponding experimental values. Since ignition delay is essentially kinetically controlled in homogeneous systems, the quality of the employed reaction mechanism is therefore confirmed by this study.

In Fig. 2, τ is plotted as a function of T_0. As expected, a strong decrease of τ for increasing T_0 is observed. It is interesting to note that the auto-ignition delay from zero-dimensional (homogeneous) and one-dimensional computations all collapse on a single value for a given T_0. This also confirms the choice of the employed stiffness parameter.

Also shown in Fig. 2 are the auto-ignition delay from selected laminar and turbulent H_2-air spherical premixed kernels computations in both two (setup *S2D*) and three (setup *S3D*) dimensions for different initial kernel temperatures. The computed induction times for both flow conditions are much higher

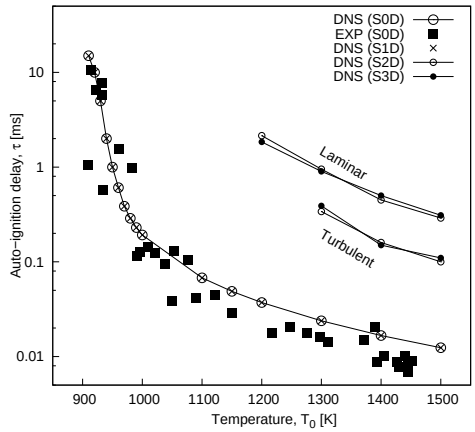

Figure 2: Self-ignition delay of stoichiometric H_2-air mixtures under laminar conditions versus initial temperature, together with experimental data [26, 27]. Results obtained for premixed kernels involving a hot region in either 2D or 3D are shown as well for comparison and later discussion.

compared with those from the homogeneous case for any given T_0, even if the slope of the curve stays similar. This is expected, since additional physical effects for curved flames are introduced and modify transport processes. Considering now each pair for the laminar or turbulent computations at any given T_0 value, the ignition delay obtained in 2D and 3D cases always show negligible differences, both with and without turbulence (Fig. 2). This demonstrates that, while the initial flame setup (curved vs. planar flames) strongly influences the results, the dimensionality (2D vs. 3D) for a given setup does not impact the ignition delay, even for turbulent computations. Hence, 2D DNS are enough to describe with a sufficient accuracy the ignition probability, as done by other groups [13]. In this manner, systematic studies become possible. Furthermore, Fig. 2 is a first indication that turbulence leads to a reduction of the mean ignition delay, as discussed later in more details.

Ignition under turbulent conditions

Adding now time-decaying isotropic turbulence for various turbulent intensities, the influence of turbulence on the probability of self-ignition events of premixed hydrogen-air mixtures can be quantified. For this purpose, only setup *S2D* (initially spherical kernels computed by 2D DNS) is considered in what follows. As documented in Table 1, the turbulence intensity u'/s_L is varied from 1.25 to 10.0 for a constant initial kernel radius of $R_0 = 3.0$ mm.

The impact of turbulence on the initially laminar kernel is illustrated in Fig. 3, where slides of the temperature field at three different time instances are displayed for selected realizations of *Case 2* ($u'/s_L = 2.5$) and *Case 14* ($u'/s_L = 10.0$). The first scenario, where the turbulence is relatively mild (left column, Fig. 3(a,c,e)) leads to a successful auto-ignition event. In the right column (Fig. 3(b,d,f)) intense turbulence leads to a misfire. The turbulence intensity is in this last case so intense that it ultimately leads to a complete quenching of the reactions. As the turbulence increasingly wrinkles the kernel with time, the maximum temperature in the domain is then observed to drop from 1300 K to well below 800 K with increasing time.

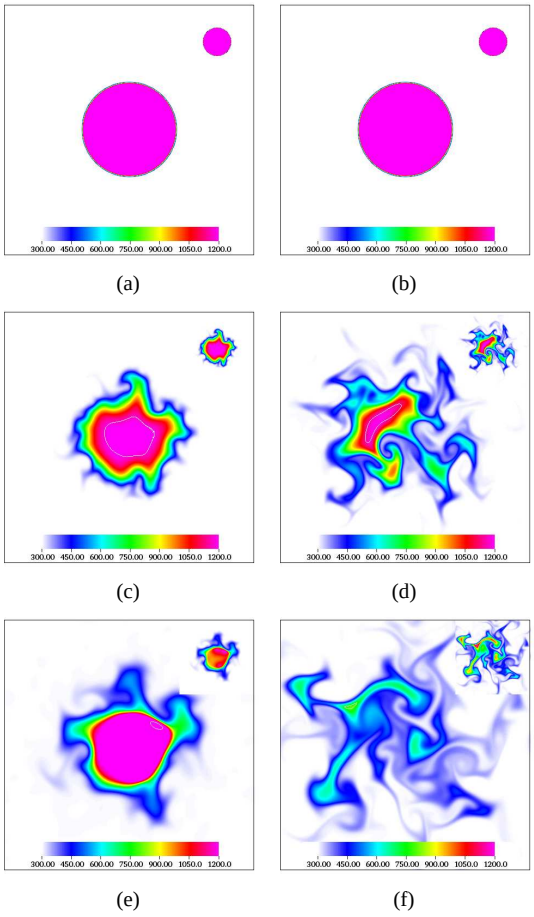

Figure 3: Auto-ignition of stoichiometric premixed H_2-air kernels under turbulent conditions: Temporal evolution of temperature field during a (a,c,e) successful auto-ignition and (b,d,f) misfire event for $u'/s_L = 2.5$ and $u'/s_L = 10.0$, respectively. The color scale is fixed for the main plots while the inlaid subplots in the upper-right corner show the same results with a min-max color scale.

For a given turbulence intensity, each of the simulated turbulent cases has been finally repeated up to twenty times, corresponding to independent realizations for a fixed value of u'/s_L. The time-dependent profiles of the maximum temperature in the computational domain for the laminar and first eleven turbulent computations at three different turbulence intensities, $\mathrm{Re}_t = 146$ (*Case 2*), $\mathrm{Re}_t = 438$ (*Case 10*) and $\mathrm{Re}_t = 584$ (*Case 14*) are exemplified in Fig. 4. The obtained auto-ignition delays are shown for selected cases in Table 2, including the mean value for each u'/s_L. With these initial parameters/conditions, the unperturbed setup will always ignite at $\tau_0 = 2.14$ ms and is hereby taken as a reference case (*case 0*, shown as bold line in Fig. 4). Figure 4(a) shows a case for which corresponding H_2-air kernels will always ignite. Its mean auto-ignition delay $\tau_{mean} = 2.16$ ms is very slightly higher than the laminar ignition delay, $\tau_0 = 2.14$ ms. Note, however, that for such conditions a single turbulent realization might deliver either a faster or a shorter ignition delay compared to the laminar case, as illustrated in Fig. 4(a). Prior to auto-ignition, the

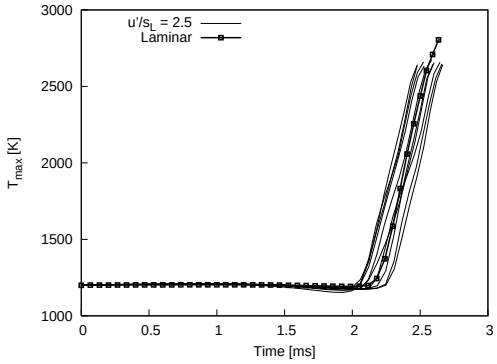

(a) Re_t = 146 (*Case 2*)

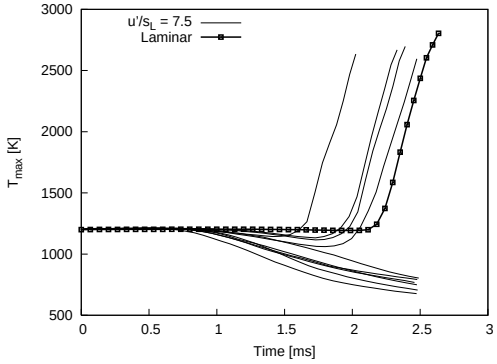

(b) Re_t = 438 (*Case 10*)

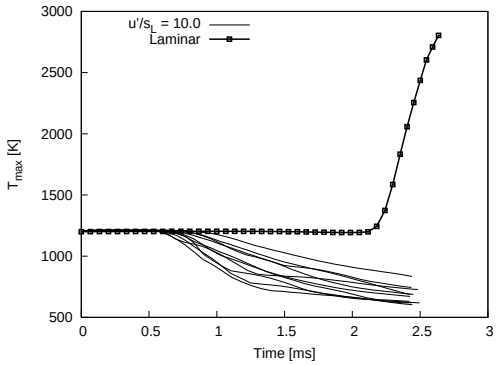

(c) Re_t = 584 (*Case 14*)

Figure 4: Auto-ignition of stoichiometric premixed H_2-air kernels under turbulent conditions: Temporal evolution of maximum temperature within the computational domain for the laminar case and first eleven turbulent realizations, initially at T_0 = 1200 K, R_0 = 3.0 mm and one atmosphere.

maximum temperature drops very slightly before rising again, initially with a similar exponential shape to the laminar case. On average, this first drop in maximum temperature tends to increase with Re_t. For all intermediate turbulence levels (cases where $3.1 \leq u'/s_L < 8.1$), the turbulent flow ignites in average faster than the laminar reference case. For most cases, all turbulent realizations ignite –when successful– faster than the laminar realization, as shown for instance in Fig. 4(b), confirming observations from the literature [25, 10]. The mean ignition delay under turbulent conditions (averaged from at least eleven realizations), τ_{mean} is shown in Fig. 5(a) as a function of u'/s_L, with error bars representing the minimum and maximum ignition delay for the first eleven repetitions at a given u'/s_L. A general decrease of τ_{mean} with the turbulence intensity can be observed. From this figure, it can be seen that weak turbulent fluctuations will first increase slightly the average ignition delay. Too intense turbulence will result in a systematic misfire (Fig. 4(c)). In between, the ignition occurs increasingly rapidly but with a decreasing probability.

Cases	*2*	*4*	*6*	*8*	*9*	*10*	*12*
Run 1	2.15	2.01	1.90	2.00	∞	∞	∞
Run 2	2.20	2.04	∞	1.96	∞	2.02	∞
Run 3	2.14	1.94	2.15	∞	∞	1.68	∞
Run 4	2.09	2.04	1.97	∞	1.92	∞	∞
Run 5	2.10	2.15	2.17	∞	1.97	∞	∞
Run 6	2.11	∞	∞	1.93	∞	∞	∞
Run 7	2.30	1.83	∞	2.14	∞	∞	1.74
Run 8	2.29	2.03	1.75	1.99	1.84	2.09	∞
Run 9	2.09	1.94	∞	∞	∞	∞	∞
Run 10	2.24	2.11	1.99	∞	∞	1.97	∞
Run 11	2.10	2.07	2.23	1.79	∞	∞	∞
Mean	2.16	2.02	2.02	1.97	1.91	1.94	1.74

Table 2: Auto-ignition of stoichiometric premixed H_2-air kernels under turbulent conditions: Induction times for kernels initially at T_0 = 1200 K, R_0 = 3.0 mm and one atmosphere. Entries with an infinity symbol (∞) refer to a misfire event.

The probability of a successful auto-ignition event P_i is shown in Fig. 5(b) as a function of u'/s_L. For $u'/s_L \leq 3.1$, the ignition probability remains constant at $P_i = 1.0$. This is directly followed by a region of linear decrease with increasing u'/s_L, up to $u'/s_L = 5.6$, from where this monotonic dependency is lost considering only eleven realizations, as with the τ_{mean} profiles. In order to check this evolution, additional realizations have been afterwards included for those specific u'/s_L values for which a non-uniform trend in P_i was first observed. The P_i values computed from sixteen realizations are shown as well in Fig. 5(b), and lead back to a strictly decreasing and monotonic profile up to $u'/s_L = 8.1$. For this last value, and due to a very high probability of misfire, even sixteen runs are not enough. Increasing the number of realizations to twenty, it was finally possible to establish a monotonic profile for the entire spectrum of u'/s_L values. This interesting observation shows that a relatively high number of repetitions might be required under certain conditions in order to get a consistent trend concerning auto-ignition probability and delay at high turbulence levels.

Conclusions

Direct Numerical Simulations of atmospheric H_2-air mixtures have been performed under stoichiometric conditions in order to investigate the probability of successful (or misfired) auto-ignition events under laminar and turbulent conditions. Besides the influence of the mixture equivalence ratio on the auto-ignition delay, a critical self-ignition initial temperature ($T_{0,c}$) and initial hot kernel radius ($R_{0,c}$) have been identified. In one-dimensional configurations, $T_{0,c}$ = 910 K and $R_{0,c}$ =

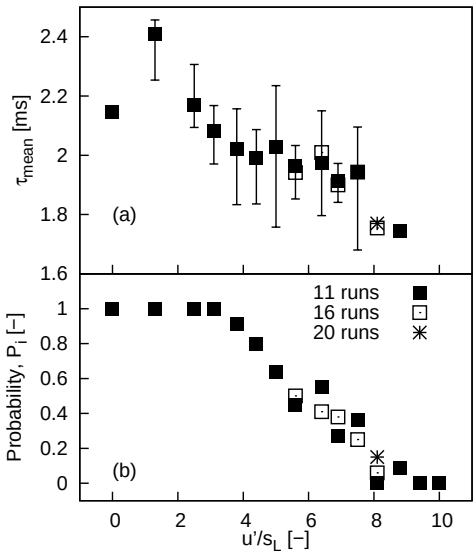

Figure 5: Auto-ignition of stoichiometric premixed H_2-air kernels under turbulent conditions: (a) Mean auto-ignition delay and (b) auto-ignition probability versus turbulence intensity (u'/s_L) for initial conditions $T_0 = 1200$ K, $R_0 = 3.0$ mm and one atmosphere. The laminar case is plotted for $u'/s_L = 0$.

0.3 mm, while in spherical kernels with the same mixture composition, first ignition events are recorded for $T_{0,c} = 1200$ K and $R_{0,c} = 1.8$ mm. A similar evolution is observed in the computed auto-ignition delays. Moreover, induction times from two-dimensional calculations prove to be extremely close to those from three-dimensional computations under the same conditions, so that systematic studies can be carried out using 2D DNS. The induction times computed using the employed numerical and physicochemical models show a very good agreement with available experimental data.

Self-ignition scenarios in the turbulent regime considering homogeneous isotropic turbulence are then considered to characterize the influence of the interaction between kinetics and heat transport processes while varying the turbulent Reynolds number. It is observed that all spherical stoichiometric premixed kernels of H_2-air with $T_0 \geq T_{0,c}$ and $R_0 \geq R_{0,c}$ will successfully auto-ignite in a turbulent environment with turbulence intensities $u'/s_L \leq 3.1$. Beyond this intensity, the mean auto-ignition delay becomes shorter than the laminar one for all successful ignitions. At the other extreme, a misfire appears to be inevitable for $u'/s_L \geq 9.4$. By repeating the DNS realizations up to twenty times, the probability of successful ignition events is found to decrease monotonically and almost linearly with u'/s_L when this value exceed roughly 3, until getting a systematic misfire.

Future studies will consider the possible influence of the turbulence length scale. Additionally, it is important to understand the underlying physical and chemical processes leading to the reported observations.

Acknowledgements

The financial support of the German Research Council (DFG) within the project *FOR*1447 "Physicochemical-based models for the prediction of safety-relevant ignition processes" is gratefully acknowledged.

References

[1] B. Lewis, G. von Elbe, Combustion, Flames and Explosions of Gases, Academic Press Inc, 3rd edition, 1987.
[2] C. K. Law, in: N. Peters, B. Rogg (Eds.), Reduced Kinetic Mechanisms for Applications in Combustion Systems, volume 15 of *Lecture Notes in Physics monographs*, Springer-verlag, 1993, pp. 15–26.
[3] T. Hasegawa, A. Arai, S. Kadowaki, S. Yamaguchi, Combust. Sci. Tech. 84 (1992) 1–13.
[4] M. Baum, T. Poinsot, Combust. Flame 106 (1995) 19–39.
[5] T. Poinsot, S. Candel, A. Trouvé, Prog. Energy Combust. Sci. 21 (1996) 531–576.
[6] T. Poinsot, D. Veynante, Theoretical and Numerical Combustion, R. T. Edwards, 2nd edition, 2005.
[7] C. Kaminski, J. Hult, M. Alden, S. Lindenmaier, A. Dreitzler, U. Maas, M. Baum, Proc. Combust. Inst. 28 (2000) 399–405.
[8] J. Hult, S. Gashi, N. Chakraborty, M. Klein, K. Jenkins, R. Cant, C. Kaminski, Proc. Combust. Inst. 31 (2007) 1319–1326.
[9] M. Klein, N. Chakraborty, R. Cant, Flow Turb. Comb. 81 (2008) 583–607.
[10] N. Chakraborty, E. Mastorakos, S. Cant, Combust. Sci. Tech. 179 (2007) 293–317.
[11] R. Sankaran, E. Hawkes, H. Chen, T. Lu, C. Law, Proc. Combust. Inst. 31 (2007) 1291–1298.
[12] H. Reddy, J. Abraham, Fuel 89 (2010) 3262 – 3271.
[13] C. Yoo, T. Lu, J. H. Chen, C. K. Law, Combustion and Flame 158 (2011) 1727 – 1741.
[14] G. Bansal, H. G. Im, Combustion and Flame 158 (2011) 2105 – 2112.
[15] D. Thévenin, F. Behrendt, U. Maas, B. Przywara, J. Warnatz, Comput. Fluids 25 (1996) 485–496.
[16] G. Fru, G. Janiga, D. Thévenin, Flow Turb. Comb. 88 (2012) 451–478.
[17] A. Honein, P. Moin, J. Comput. Phys. 201 (2004) 531–545.
[18] M. Baum, T. Poinsot, D. Thévenin, J. Comput. Phys. 116 (1995) 247–261.
[19] U. Maas, J. Warnatz, Combust. Flame 74 (1988) 53–69.
[20] A. Ern, V. Giovangigli, Multicomponent Transport Algorithms, Lecture Notes in Physics, New series Monographs m24, 1994.
[21] J. Hirschfelder, C. Curtiss, R. Bird, Molecular Theory of Gases and Liquids, New York: Wiley, 1954.
[22] H. Shalaby, D. Thévenin, Flow Turb. Comb. 84 (2010) 357–367.
[23] E. Mastorakos, A. P. da Cruz, T. Baritaud, T. Poinsot, Combust. Sci. Tech. 125 (1997) 243–282.
[24] H. G. Im, J. H. Chen, C. K. Law, Proc. Combust. Inst. 27 (1998) 1047–1056.
[25] R. Hilbert, D. Thévenin, Combust. Flame 128 (2002) 22–37.
[26] I. Momtchiloff, E. Taback, R. Buswell, Proc. Combust. Inst. 9 (1962) 220–230.
[27] W. Laster, E. Sojka, Jet Propu. 4 (1989) 385–390.